

CONFORMATIONAL ANALYSIS. 49.<sup>1</sup> A COMPLETE CONFORMATIONAL ANALYSIS OF THE  
TRANS-2-( $\alpha$ -HYDROXYBENZYL)THIANE SULFOXIDES<sup>#</sup>

Ernest L. Eliel,<sup>\*</sup> Edward M. Olefirowicz,<sup>2</sup> Maria T. Alvarez,<sup>3</sup>

Derek J. Hodgson<sup>4</sup>, and Debra K. Towle

W.R. Kenan, Jr. Laboratories, Department of Chemistry

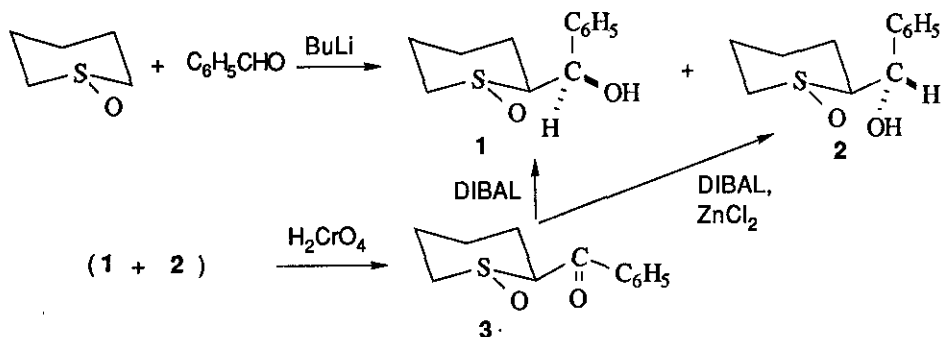
University of North Carolina, Chapel Hill, NC 27599-3290, U.S.A.

*Abstract* - The relative stereochemistry of the title compounds has been determined by X-ray structure analysis of the R\*S\*R\* diastereomer. The compound C<sub>12</sub>H<sub>16</sub>O<sub>2</sub>S crystallizes in the monoclinic space group P2<sub>1</sub>/c with  $a = 14.161(8)$ ,  $b = 10.135(4)$ ,  $c = 15.999(7)$ ,  $\beta = 97.17(4)^\circ$ , and  $V = 2278(3)\text{\AA}^3$ . There are two crystallographically independent molecules in the cell, and a total of eight molecules per cell. Both independent molecules are present as the same diastereomer, but they undergo two different forms of intermolecular hydrogen bonding. Infrared analysis of this isomer in dilute solution shows intramolecular hydrogen bonding which is absent in the crystal. Both isomers were analyzed by proton and <sup>13</sup>C nmr spectroscopy and their conformational energy profiles as a function of the Ph-C(6)-C(1)-H(1) torsion angle were assessed by MMP2 force field calculations. The energy profile shows an interesting interplay between torsional and hydrogen-bonding forces.

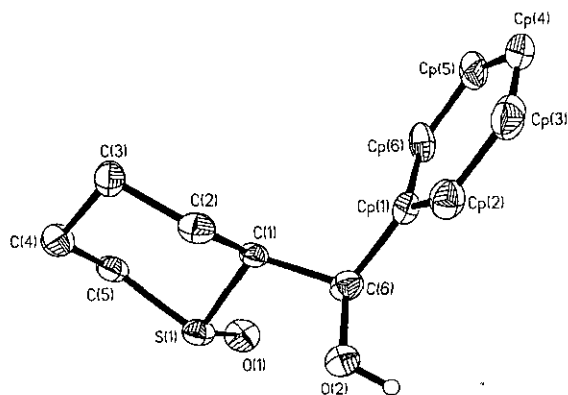
#### INTRODUCTION

In connection with another problem we had occasion to synthesize the two equatorial sulfoxides  $\overset{1}{\sim}$  and  $\overset{2}{\sim}$  epimeric at the  $\alpha$ -carbon, as well as their axial sulfoxide isomers. A mixture of racemic  $\overset{1}{\sim}$  and  $\overset{2}{\sim}$  was obtained by condensing the lithium derivative of pentamethylene sulfoxide with benzaldehyde (Scheme 1);  $\overset{1}{\sim}$  was isolated from the resulting mixture of trans sulfoxides by crystallization from ethanol. To obtain  $\overset{2}{\sim}$ , the crude carbinol product was oxidized to ketone  $\overset{3}{\sim}$  with aqueous chromic acid in an ether-tetrahydrofuran mixture and  $\overset{3}{\sim}$  was then reduced with

<sup>#</sup> Dedicated to Professor Derek H.R. Barton on the occasion of his 70th birthday



diisobutylaluminum hydride - zinc chloride<sup>5</sup> to give predominantly  $\underline{2}$ . (Reduction of  $\underline{3}$  with diisobutylaluminum hydride alone gave very largely  $\underline{1}$ .) The trans stereochemistry of ketone  $\underline{3}$  was established by comparing its <sup>13</sup>C nmr spectrum with that of the cis isomer<sup>6</sup> and noting that the ring carbons of the cis isomer (axial sulfoxide!) uniformly resonated at higher field; this is particularly true for the carbons gamma to the sulfoxide oxygen: C(2): cis, 18.7, trans, 24.9 ppm; C(4), cis, 15.4, trans, 21.6 ppm. However, it was not clear, a priori, which isomer was  $\underline{1}$  and which  $\underline{2}$ ; this problem was solved by X-ray crystallography of  $\underline{1}$ , mp 183-184°C, which showed it to be the R\*S\*R\* isomer;  $\underline{2}$  must therefore be R\*S\*S\*. (Incidentally, the X-ray structure also corroborates the trans-diequatorial arrangement of the ring substituents in  $\underline{1}$ .)



View of one crystallographically independent molecule [Molecule I] of  $C_{12}H_{16}O_2S$ . The molecule shown here is the R[S(1)],S[C(1)],R[C(6)] enantiomorph, but in this centrosymmetric space group there is an equal distribution of the enantiomeric S[S(1)],R[C(1)],S[C(6)] form. All hydrogens, except the hydroxy hydrogen atom, are omitted for clarity.

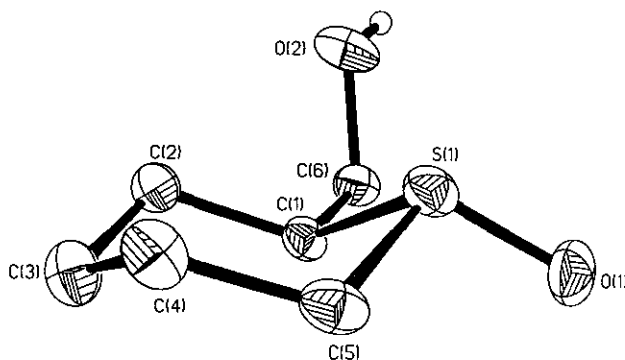
Figure 1

## X-RAY DIFFRACTION, INFRARED AND NMR SPECTROSCOPY

X-Ray Crystallography - Description of Structure. There are two non-symmetry related molecules in the unit cell of  $\underline{1}$ . Both of these molecules are present as the  $\underline{R[S(1)],S[C(1)],R[C(6)]}$  diastereomer and (necessarily, in this centrosymmetric crystal) their enantiomeric  $\underline{S[S(1)],R[C(1)],S[C(6)]}$  forms. A view of Molecule I is given in Figure 1. Molecule II is substantially similar to this, as can be seen in the tables of bond lengths and bond and torsional angles given in Tables 1, 2 and 3, respectively.

TABLE 1. Internuclear Distances ( $\text{\AA}$ ) in  $\text{C}_{12}\text{H}_{16}\text{O}_2\text{S}$ 

Molecule I		Molecule II	
S(1) - O(1)	1.504(3)	S(2) - O(3)	1.503(2)
S(1) - C(1)	1.807(4)	S(2) - C(21)	1.815(3)
S(1) - C(5)	1.793(4)	S(2) - C(25)	1.791(4)
C(1) - C(2)	1.534(5)	C(21) - C(22)	1.517(5)
C(1) - C(6)	1.533(5)	C(21) - C(26)	1.550(5)
C(2) - C(3)	1.542(5)	C(22) - C(23)	1.515(5)
C(3) - C(4)	1.514(5)	C(23) - C(24)	1.510(5)
C(4) - C(5)	1.516(5)	C(24) - C(25)	1.541(6)
C(6) - O(2)	1.415(4)	C(26) - O(4)	1.416(4)
C(6) - CP1	1.519(5)	C(26) - CP7	1.518(5)
CP1 - CP2	1.389(6)	CP7 - CP8	1.408(5)
CP1 - CP6	1.380(5)	CP7 - CP12	1.349(5)
CP2 - CP3	1.385(6)	CP8 - CP9	1.382(6)
CP3 - CP4	1.360(6)	CP9 - CP10	1.357(6)
CP4 - CP5	1.409(6)	CP10 - CP11	1.386(6)
CP5 - CP6	1.353(6)	CP11 - CP12	1.407(6)
O(2) - H(O2)	0.80(4)	O(4) - H(O4)	0.68(4)



View of the heterocyclic ring portion of  $\text{C}_{12}\text{H}_{16}\text{O}_2\text{S}$ . The phenyl ring and hydrogens have been omitted for clarity.

Figure 2

TABLE 2. Internuclear Angles (deg.) in  $C_{12}H_{16}O_2S$ 

Molecule I		Molecule II	
O(1)-S(1)-C(1)	107.3(1)	O(3)-S(2)-C(21)	106.7(1)
O(1)-S(1)-C(5)	105.0(2)	O(3)-S(2)-C(25)	105.8(1)
C(1)-S(1)-C(5)	95.0(2)	C(21)-S(2)-C(25)	97.3(2)
S(1)-C(1)-C(2)	109.4(2)	S(2)-C(21)-C(22)	110.2(2)
S(1)-C(1)-C(6)	110.4(2)	S(2)-C(21)-C(26)	107.3(2)
C(2)-C(1)-C(6)	113.2(3)	C(22)-C(21)-C(26)	114.7(3)
C(1)-C(2)-C(3)	111.4(3)	C(21)-C(22)-C(23)	113.4(3)
C(2)-C(3)-C(4)	111.8(3)	C(22)-C(23)-C(24)	113.0(3)
C(3)-C(4)-C(5)	111.7(3)	C(23)-C(24)-C(25)	112.3(3)
C(4)-C(5)-S(1)	113.5(3)	C(24)-C(25)-S(2)	109.7(3)
C(1)-C(6)-O(2)	107.6(3)	C(21)-C(26)-O(4)	105.9(3)
C(1)-C(6)-CP1	110.4(3)	C(21)-C(26)-CP7	109.6(3)
O(2)-C(6)-CP1	113.6(3)	O(4)-C(26)-CP7	110.9(3)
C(6)-CP1-CP2	122.2(4)	C(26)-CP7-CP8	118.0(4)
C(6)-CP1-CP6	120.6(4)	C(26)-CP7-CP12	123.3(4)
CP2-CP1-CP6	117.3(4)	CP8-CP7-CP12	118.6(4)
CP1-CP2-CP3	121.0(4)	CP7-CP8-CP9	119.5(4)
CP2-CP3-CP4	121.3(4)	CP8-CP9-CP10	121.1(4)
CP3-CP4-CP5	117.4(4)	CP9-CP10-CP11	120.5(4)
CP4-CP5-CP6	121.2(4)	CP10-CP11-CP12	118.0(4)
CP1-CP6-CP5	121.8(4)	CP7-CP12-CP11	122.1(4)

The bond lengths in the molecules (Table 1) are unremarkable. The six-membered heterocyclic ring is well described as a chair, as is shown in Figure 2 and can be deduced from the torsional angles in Table 3. Thus, atoms S(1), C(2), C(3), C(5) are approximately coplanar [maximum deviation  $0.025\text{\AA}$ ], while atom C(1) lies  $0.844\text{\AA}$  above this plane and atom C(4) sits  $0.686\text{\AA}$  below it.

The major difference between the two independent molecules is in their hydrogen bonding. As is shown in Figure 3, each Molecule I is involved in intermolecular hydrogen bonding with two other molecules I along the  $2_1$  screw axis, leading to a hydrogen bonded chain of molecules I along the  $b$ -axis. The O(2)...O(1a) distance and O(2)-H(2)...O(1a) angle associated with these interactions are  $2.804(8)\text{\AA}$  and  $168(2)^\circ$ , respectively. The hydrogen bonding in Molecule II, shown in Figure 4, involves pairwise interactions across the inversion center. The O(4)...O(3a) distance and O(4)-H(4)...O(3a) angle in this interaction are  $2.696(8)\text{\AA}$  and  $163(2)^\circ$ , respectively.

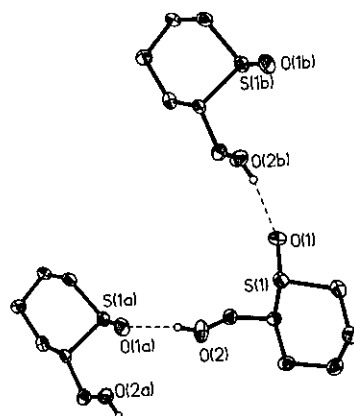
The proton nmr spectrum of  $\underline{1}$  displays a 3.0 Hz coupling constant between the carbinol hydrogen H(1) and H(6). This corresponds to a gauche conformation of these protons and suggests that  $\underline{1}$  exists in either the  $\omega = 180^\circ$  [ $C_6H_5/H(1)$  torsion angle] conformation B or the  $\omega = 60^\circ$  conformation C in Fig. 5 or as a mixture of the two. The  $\omega = 60^\circ$  structure is close to that found by X-ray diffraction ( $\omega = 54^\circ$  and  $46^\circ$  in the two independent molecules) but, whereas both B and C

TABLE 3. Selected Torsional Angles

Molecule I				
Atom 1	Atom 2	Atom 3	Atom 4	Angle
O(2)	C(6)	C(1)	S(1)	-68.4
O(2)	C(6)	C(1)	C(2)	54.5
CP1	C(6)	C(1)	S(1)	167.1
CP1	C(6)	C(1)	C(2)	-69.9
C(6)	C(1)	S(1)	O(1)	-66.4
C(6)	C(1)	S(1)	C(5)	-173.8
C(6)	C(1)	C(2)	C(3)	169.3
C(1)	C(2)	C(3)	C(4)	61.4
C(2)	C(3)	C(4)	C(5)	-57.6
C(3)	C(4)	C(5)	S(1)	62.7
C(4)	C(5)	S(1)	C(1)	-60.1
C(4)	C(5)	S(1)	O(1)	-169.4
C(5)	S(1)	C(1)	C(2)	61.0
O(1)	S(1)	C(1)	C(2)	168.4

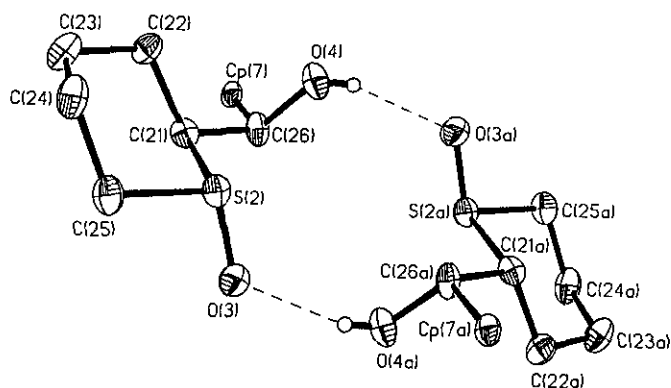
  

Molecule II				
Atom 1	Atom 2	Atom 3	Atom 4	Angle
O(4)	C(26)	C(21)	S(2)	-65.5
O(4)	C(26)	C(21)	C(22)	57.3
CP7	C(26)	C(21)	S(2)	174.9
C(26)	C(21)	S(2)	O(3)	-66.7
C(26)	C(21)	S(2)	C(25)	-175.6
C(26)	C(21)	C(22)	C(23)	177.2
C(21)	C(22)	C(23)	C(24)	58.4
C(22)	C(23)	C(24)	C(25)	-59.1
C(23)	C(24)	C(25)	S(2)	64.2
C(24)	C(25)	S(2)	C(21)	-59.8
C(24)	C(25)	S(2)	O(3)	-169.5
C(25)	S(2)	C(21)	C(22)	58.9
O(3)	S(2)	C(21)	C(22)	167.8



The hydrogen bonding scheme in Molecule I. Phenyl rings are omitted.

Figure 3



The hydrogen bonding scheme in Molecule II. Phenyl rings are omitted

Figure 4

would seem to provide opportunity for intramolecular hydrogen bonding, none was evidenced in the crystal. (It is, of course, common for crystalline solids to engage in intermolecular in preference to intramolecular hydrogen bonding.)

This matter was further explored by hydrogen bonding studies in solution by infrared spectroscopy (Table 4). It is clear that at high concentrations inter- as well as intramolecular hydrogen bonding exists, but that only intramolecular hydrogen bonding remains at the lowest concentration attained.<sup>7</sup>

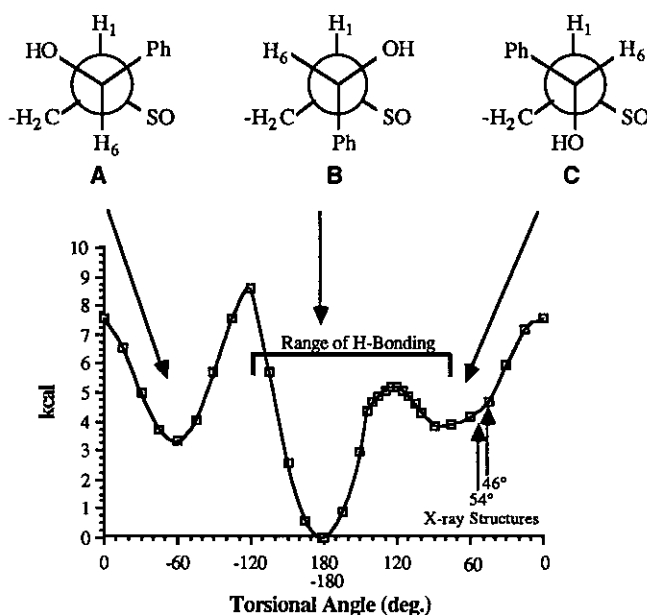
TABLE 4. Infrared data of  $\frac{1}{\nu}$

Concentration (M)	( $\text{cm}^{-1}$ )	Type of H-bonding
$1 \times 10^{-1}$	3615	Intramolecular
	3500-3200	Intermolecular
$2 \times 10^{-2}$	3612	Intramolecular
	3500-3200	Intermolecular
$5 \times 10^{-3}$	3612	Intramolecular

#### MOLECULAR MECHANICS CALCULATIONS

To gain a better understanding of the hydrogen bonding situation in  $\frac{1}{\nu}$  we performed molecular mechanics calculations using Allinger's MMP2(85) program.<sup>8</sup> Since in  $\frac{1}{\nu}$  there is opportunity for independent rotation about three bonds [C(6)-C(1), C(6)-O and C(6)-Ph], and since a complete exploration of all three rotational circuits at once would have required an excessive amount of computer time, we used the dihedral angle drive option to rotate the exocyclic [C(6)-C(1)] bond from different starting points and in different directions, allowing the C(6)-OH and C(6)-Ph bonds to rotate spontaneously so as to minimize the energy for each chosen value of the C(6)-C(1) bond

from different starting points and in different directions, allowing the C(6)-OH and C(6)-Ph bonds to rotate spontaneously so as to minimize the energy for each chosen value of the C(6)-C(1) torsion angle. In this way the potential energy curve shown in Fig. 5 was obtained. While the calculation refers to isolated molecules in the gas phase it probably also approximates the situation in dilute solution in a non-polar solvent which is quite different from that in the crystal.



Calculated potential energy of  $\tilde{1}$  as a function of the H(1)-C(1)-C(6)-Ph torsional angle

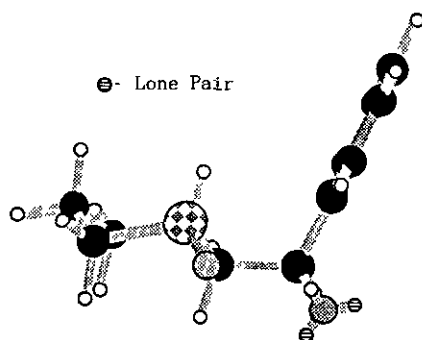
Figure 5

#### DISCUSSION

The global minimum for  $\tilde{1}$  occurs at  $\omega = -179.5^\circ$ , very close to the staggered conformation B. The calculated structure is shown in Fig. 6; the S-O...H-O distance in this structure is  $2.12\text{\AA}$ , well within the distance for a hydrogen bond<sup>9</sup> as confirmed by IR; the H(1)/H(6) torsion angle of  $59.9^\circ$  is compatible with the observed 4.2 Hz coupling constant. There are two secondary minima, one at  $\omega = -59.6^\circ$  (i.e. very close to staggered), 3.31 kcal/mol above the  $179^\circ$  minimum, and one at  $84.5^\circ$ , substantially displaced from the staggered position (by  $24.5^\circ$ ), at an energy of 3.75 kcal/mol above the minimum.

The energy barrier between the  $180^\circ$  and  $-60^\circ$  minima is very high (8.6 kcal/mol above the lower and 5.3 kcal/mol above the higher minimum). This barrier corresponds to SO/Ph eclipsing which may be quite severe, even though the plane of the phenyl ring is perpendicular to the plane passing

through C(6), C(1) and C(4) (see Fig. 6). The potential curve is particularly steep in the  $\omega = -150^\circ$  to  $-120^\circ$  region, rising by nearly 6 kcal. In fact, just between  $\omega = -135^\circ$  and  $\omega = -120^\circ$ , the energy rises by nearly 3 kcal/mol. We have examined the conformations corresponding to these torsion angles in more detail and found the following situation: At  $\omega = -135^\circ$  the S-O...H-O distance is 2.26Å, well within hydrogen bonding distance. But as the absolute value of  $\omega$  decreases to  $-120^\circ$  the S-O...H-O distance increases rapidly to 3.14Å, a distance which no longer permits hydrogen bonding. The corresponding calculated energy of 8.99 kcal/mol can actually be decreased to 8.61 kcal/mol by driving the H-O-C(6)-C(1) torsion angle so as to rotate the O-H away from the S-O.



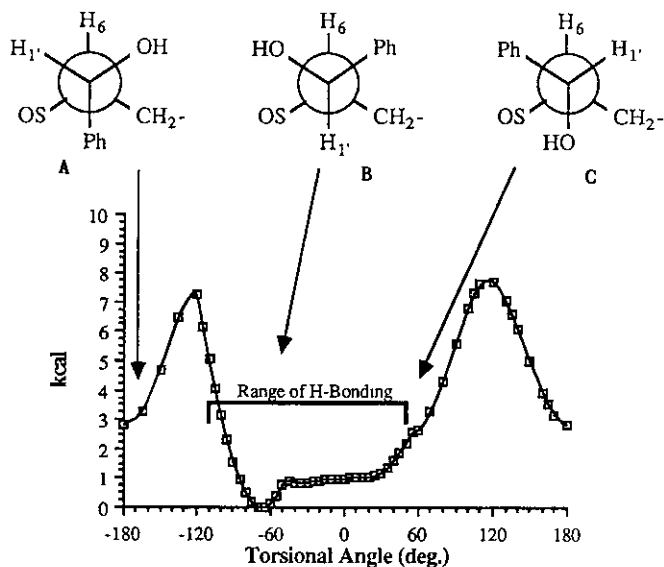
Optimal Conformation of  $\tilde{1}$  (calculated)

Figure 6

The range of hydrogen bonding as obtained from the MMP2(85) program<sup>9</sup> is marked in Fig. 5. It may be noted that the energy barrier between B and C, near  $120^\circ$ , is relatively flat at 5 kcal/mol, only 1.25 kcal/mol above C. Although this barrier corresponds to Ph/CH<sub>2</sub> eclipsing, its energy level is evidently reduced by a very strong S-O...H-O hydrogen bond as the OH eclipses SO at the barrier. Earlier work<sup>7</sup> had shown that an -S-O...H-O-intramolecular hydrogen bond may contribute more than 2.6 kcal/mol to the stabilization of a conformation so bonded.

The displacement of energy minimum C from the staggered  $60^\circ$  to  $84.5^\circ$  (vide supra) can now be explained also in terms of intramolecular hydrogen bonding. While there must be substantial eclipsing energy (torsional and possibly also steric) at  $\omega = 84.5^\circ$ , this is obviously more than compensated by the S-O...H-O hydrogen bond which is maintained at  $\omega = 84.5^\circ$  but ruptures at  $\omega = 60^\circ$  (cf. Fig. 5). It is probably the weakening of this hydrogen bond which makes conformation C so much less stable than B. Examination of models shows that the geometry for S-O...H-O hydrogen bonding is considerably more favorable in B than in C. The counterplay of increased staggering and a decreasingly strong hydrogen bond makes the minimum at C rather shallow.



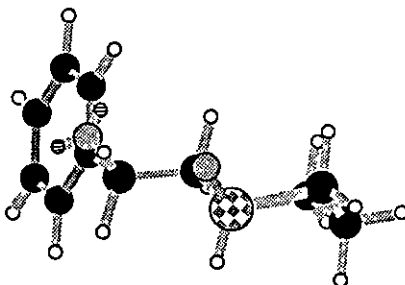


Potential energy of  $\tilde{2}'$  as a function of the H(6)-C(6)-C(1)-Ph torsion angle

Figure 7

The X-ray structures, marked in Fig. 5, lie very slightly above the secondary energy minimum C. Since there are obviously strong intermolecular forces in the crystal which cannot be assessed by molecular mechanics calculations of isolated molecules, little can be said about the crystal structure in terms of molecular mechanics except to point out that the absence of intramolecular hydrogen bonding would clearly tend to equalize the energy levels of B and C or even make C more stable than B.

Compound  $\tilde{2}'$ 's calculated energy profile is shown in Fig. 7. The H(6)/H(1') coupling constant in proton nmr here is 7.7 Hz suggesting a considerable contribution of the  $-60^\circ$  conformation (Fig. 7) in which these protons are anti to each other. Calculation, in fact, indicates a very flat energy level between  $-80^\circ$  and  $+40^\circ$ , with the global minimum at  $\omega = -67.9^\circ$  and a secondary minimum at  $\omega = \pm 180^\circ$ . The global minimum, shown in Fig. 8, is stabilized by hydrogen bonding; the secondary minimum at  $\pm 180^\circ$ , 2.9 kcal/mol above the global minimum, is not. The minimum normally seen at  $+60^\circ$  (staggered conformation) is absent. The very flat region from  $\omega = -45^\circ$  to  $+45^\circ$  suggests that in this region the eclipsing (maximal as  $\omega$  passes through  $0^\circ$ ) and the hydrogen bonding (also maximal at  $0^\circ$ ) hold each other in balance. However, the hydrogen bond ruptures before the  $60^\circ$  staggered conformation C is reached and as result (and perhaps also because of unfavorable gauche interactions in C) there is no energy minimum at C nor is there an energy barrier between



Optimal conformation of  $\underline{2}$  (calculated)

Figure 8

B and C. A and B are separated by barriers of 7.24 kcal/mol (at  $-120^\circ$ ) and 7.70 kcal/mol (at  $+120^\circ$ ).

In summary, in addition to assigning configurations to  $\underline{1}$  and  $\underline{2}$ , we find, by MMP2(85), an interesting interplay between eclipsing and intramolecular hydrogen bonding which leads to a very steep barrier between A and B in  $\underline{1}$  and to a vanishing B/C barrier and a vanishing minimum C in  $\underline{2}$ .

#### EXPERIMENTAL

2-(1'-Hydroxy-1'-phenyl)methylthiane sulfoxide ( $\underline{1}$ ). a) To a solution of pentamethylene sulfoxide<sup>10</sup> (13.27 g, 112.27 mmol, pre-dried under vacuum, 0.01 mm, for 12 h) in 500 ml of dry, cold ( $-78^\circ\text{C}$ ) THF under  $\text{N}_2$  was added, dropwise, 70.30 ml of 1.6 M *n*-BuLi in hexane (42.4 mmol). After stirring for 4.5 h, benzaldehyde (13.04 g, 112.3 mmol) in 200 ml dry THF was added, dropwise, over a 15 min period, at  $-78^\circ\text{C}$ . The reaction mixture was stirred overnight at  $-78^\circ\text{C}$ . Water (100 ml) and saturated  $\text{NH}_4\text{Cl}$  (50 ml) were added, the layers were separated, and the aqueous layer was extracted with  $\text{CHCl}_3$  (3x150 ml). The combined organic layers were dried ( $\text{MgSO}_4$ ) and concentrated to a cream colored solid diastereomer mixture, mp  $130$ - $135^\circ\text{C}$  (23.61 g, 94% yield).

$^1\text{H}$  Nmr ( $\delta$  ppm,  $\text{CDCl}_3$ ): 1.0-1.8 (m, 6H), 2.0 (s, 1H), 2.6-3.0 (m, 2H), 3.4 (m, 1H), 5.2 (d,  $J = 7.7$  Hz, minor isomer  $\underline{2}$ ), 5.5 (d,  $J = 3.0$  Hz, 1H, major isomer  $\underline{1}$ ) 7.3 (s, 5H).

$^{13}\text{C}$  Nmr ( $\delta$  ppm,  $\text{CDCl}_3$ ): 21.6, 22.7, 23.2, 24.1, 24.3, 24.9, 51.2, 51.3, 68.1, 68.5, 71.4, 74.4, 126.1, 127.1, 127.4, 128.0, 128.1, 128.2, 139.9, 141.4. (Signals of major isomer  $\underline{1}$  underlined).

ir ( $\tilde{\nu}$ ,  $\text{cm}^{-1}$ , Nujol): 3250 (s), 1030 (s) and others.

Recrystallization of the diastereomer mixture from 95% ethanol produced the pure diastereomer  $\underline{1}$ , mp  $183$ - $184^\circ\text{C}$ .

b) To a cold (-78°C) solution of the ketone  $\underline{3}$  (0.05 g, 0.23 mmol) in 6 ml of dry THF was added, dropwise under  $N_2$ , 0.3 ml of a 0.9 solution of DIBAL in hexanes. The mixture was stirred for 1.25 h at -78°C and then quenched at this temperature with saturated aqueous  $NH_4Cl$  solution. After separating the two layers, the aqueous layer was extracted with  $CH_2Cl_2$  (3x8 ml). The combined organic phase was dried ( $MgSO_4$ ) and concentrated to give 0.04 g (80%) of crude product, very largely isomer  $\underline{1}$ , according to proton nmr.

#### CRYSTAL STRUCTURE OF $\underline{1}$

X-ray Data Collection. The data were collected and reduced in the manner described by Graves and Hodgson.<sup>11</sup> No preliminary X-ray photographs were taken. A crystal was mounted on a glass rod in an approximate orientation parallel to its longest axis and placed on an Enraf-Nonius CAD-4 automatic diffractometer. Least squares fitting of the angular settings of twenty-five reflections indicated a monoclinic cell with  $\underline{a} = 14.161(8)$ ,  $\underline{b} = 10.135(4)$ ,  $\underline{c} = 15.999(7)\text{\AA}$ ,  $\beta = 97.17(4)^\circ$ , and  $V = 2278(3)\text{\AA}^3$ .

Diffraction data were collected on a CAD-4 diffractometer with Mo radiation [ $\lambda(\text{Mo } K_{\alpha 1}) = 0.70926\text{\AA}$ ]. A preliminary small shell data collection confirmed monoclinic symmetry. Therefore, data were collected ( $+h, +k, +l$ ) in the range of  $3 < \theta(\text{Mo}) < 24^\circ$ . Intensity checks were made on three standard reflections after every three hours of X-ray exposure time and orientation checks on the same three standard reflections were made after every 250 reflections. No systematic variation in these standards was encountered throughout data collection. These and other data collection parameters are summarized in Table 5.

TABLE 5. Crystal Data for  $C_{12}H_{16}O_2S$

F.W.	224.32	$\mu(\text{Mo } K_{\alpha}), \text{ cm}^{-1}$	2.59
space group	$P2_1/c$ (# 14)	diffractometer	CAD-4
$\underline{a}, \text{\AA}$	14.161 (8)	radiation	$\text{Mo } K_{\alpha}^a$
$\underline{b}, \text{\AA}$	10.135 (4)	data collection limit, deg.	$6 < 2\theta < 48$
$\underline{c}, \text{\AA}$	15.999 (7)	no. of unique data collected	3564
$\underline{\beta}$	97.17(4)	no. of data used, $I \geq 3\sigma(I)$	1739
$\underline{V}, \text{\AA}^3$	2278 (3)	no. of variables	279
$\underline{Z}$	8	R	0.053
$\underline{d}_{\text{-calcd}}, \text{ g cm}^{-3}$	1.308	$R_w$	0.055

<sup>a</sup>  $\lambda_{\alpha} = 0.7107$

Data reduction was carried out in the usual fashion. The intensities were assigned standard deviations according to the formula of Ibers and co-workers,<sup>12</sup> and the intensities and their standard deviations were then corrected for Lorentz-polarization effects and absorption.

Structure Solution and Refinement. Definitive systematic absences are consistent with the space group  $P2_1/c$ . There are two unique molecules per unit cell. The positions of the unique sulfur, oxygen, and many carbon atoms were found by direct methods using MULTAN.<sup>13</sup> The remaining non-hydrogen atoms and the two hydroxo-hydrogen atoms were located in difference Fourier maps. All other hydrogen atoms positions were calculated using idealized geometries at carbon with an assumed C-H distance of 0.95 Å. No positional or thermal parameters of the calculated hydrogen atoms were refined. The two hydroxo-hydrogen atoms were refined isotropically and all non-hydrogen atoms were refined anisotropically resulting in a total of 279 variables. Reflections were considered observed when  $I \geq 3\sigma(I)$ . After the final least-squares cycle the usual agreement factors  $R = \sum ||F_o| - |F_c|| / \sum |F_o|$  and  $R_w = [\sum w(|F_o| - |F_c|)^2 / \sum w F_o^2]^{1/2}$  were 0.052 and 0.055 respectively. A final difference Fourier contained no peaks greater than  $0.2e^{-3}$ . Atomic positional parameters are listed in Table 6. Hydrogen atom positions and listings of thermal parameters and observed and calculated structure amplitudes are available as supplementary material.<sup>14</sup>

trans-2-Benzoylthiane sulfoxide (3): To a solution of sulfoxyl alcohol (2.85 g, 12.71 mmol) in 290 ml of a 1:1 mixture of THF and ether was added 28.5 ml of a 2M aqueous chromic acid solution. The brown-colored mixture was stirred for 17 h. The two layers were separated, the aqueous layer was extracted with ether (3 x 40 ml), the combined organic layers were washed with sat'd aqueous  $\text{NaHCO}_3$  solution and water and was then dried ( $\text{MgSO}_4$ ) and concentrated to a yellowish solid. Recrystallization from EtOAc gave 1.78 g (65%) of white crystals which still contained 14% of the cis-β-keto sulfoxide as shown by proton nmr. Isomerically pure trans sulfoxide 3 was obtained by HPLC (silica gel) using an EtOAc-hexanes gradient, mp 124-125°C. Anal. Calcd for  $\text{C}_{12}\text{H}_{14}\text{O}_2\text{S}$ : C, 64.84; H, 6.35. Found: C, 64.79; H, 6.30.

<sup>1</sup>H Nmr ( $\delta$  ppm,  $\text{CDCl}_3$ ): 1.4-2.5 (m, 6H), 2.8-3.0 (m, 1H), 3.4-3.6 (m, 1H), 4.6 (dd,  $J = 12, 3.2$  Hz, 1H), 7.4-7.7 (m, 3H), 7.9-8.1 (m, 2H).

<sup>13</sup>C Nmr ( $\delta$  ppm,  $\text{CDCl}_3$ ): 21.0, 23.3, 26.3, 49.6, 66.1, 128.8, 129.1, 134.1, 135.6, 196.5.

DIBAL-ZnCl<sub>2</sub> reduction of trans-2-benzoylthiane sulfoxide (3): A mixture of the ketone 3 (0.04 g, 0.18 mmol) and anhydrous  $\text{ZnCl}_2$  (0.024 g, 0.18 mmol) in 8 ml of dry THF was stirred for 10 min at room temperature under  $\text{N}_2$  and an additional 0.5 h at -78°C. To the above mixture was added 1.0 ml of a 0.9 M solution of DIBAL in hexanes. The mixture was stirred for 1.5 h at -78° and then quenched at this temperature with saturated aqueous  $\text{NH}_4\text{Cl}$  solution. After separating the two

TABLE 6. Atomic Positional Parameters for  $C_{12}H_{16}O_2S$ 

ATOM	x	y	z
S(1)	0.4499(1)	0.1389(2)	0.3784(1)
S(2)	0.1520(1)	0.8473(2)	0.5335(9)
O(1)	0.4132(3)	0.0682(4)	0.2982(3)
O(2)	0.5208(3)	0.4156(5)	0.3287(3)
O(3)	0.1753(3)	0.9844(4)	0.5065(2)
O(4)	-0.0576(3)	0.8092(4)	0.4816(2)
C(1)	0.3920(4)	0.2979(6)	0.3757(4)
C(2)	0.4107(4)	0.3623(7)	0.4630(4)
C(3)	0.3610(4)	0.2861(7)	0.5286(4)
C(4)	0.3972(4)	0.1458(6)	0.5394(4)
C(5)	0.3840(4)	0.0707(6)	0.4568(4)
C(6)	0.4238(4)	0.3835(6)	0.3054(4)
CP1	0.3596(4)	0.5034(6)	0.2897(3)
CP2	0.3915(4)	0.6304(7)	0.3098(4)
CP3	0.3314(5)	0.7380(7)	0.2950(4)
CP4	0.2384(5)	0.7228(7)	0.2634(4)
CP5	0.2062(5)	0.5937(7)	0.2435(4)
CP6	0.2656(4)	0.4890(7)	0.2561(4)
C(21)	0.0941(4)	0.7640(6)	0.4404(3)
C(22)	0.0872(4)	0.6172(6)	0.4571(4)
C(23)	0.1831(5)	0.5509(6)	0.4775(4)
C(24)	0.2422(4)	0.6097(7)	0.5535(4)
C(25)	0.2618(4)	0.7577(7)	0.5423(4)
C(26)	-0.0026(4)	0.8337(6)	0.4151(3)
CP7	-0.0503(4)	0.7762(6)	0.3329(3)
CP8	-0.0188(4)	0.8191(7)	0.2574(4)
CP9	-0.0567(5)	0.7628(8)	0.1819(4)
CP10	-0.1257(5)	0.6695(7)	0.1790(4)
CP11	-0.1605(5)	0.6293(7)	0.2521(4)
CP12	-0.1215(5)	0.6870(7)	0.3287(4)
H(O2)	0.544(4)	0.449(6)	0.291(4)
H(O4)	-0.095(3)	0.851(5)	0.485(3)

layers, the aqueous layer was extracted with  $CH_2Cl_2$  (3 x 8 ml). The combined organic phase was dried ( $MgSO_4$ ) and concentrated to give 0.031 g (75%) of crude product favoring  $\underline{2}$  in 86% d.e.

Anal. Calcd for  $C_{12}H_{16}O_2S$ : C, 64.25; H, 7.19. Found: C, 64.30; H, 7.03.

$^1H$  Nmr ( $\delta$  ppm,  $CDCl_3$ ): 1.1-2.1 (m, 6H), 2.6-2.9 (m, 2H), 3.3-3.5 (m, 1H), 4.8 (s, 1H), 5.2 (d, J = 7.7 Hz, major isomer, 2), 5.5 (d, J = 3 Hz, minor isomer, 1), 7.3-7.5 (m, 5H).

$^{13}C$  Nmr ( $\delta$  ppm,  $CDCl_3$ ): 22.7, 23.0, 24.1, 24.3, 51.2, 68.0, 68.5, 71.1, 74.4, 127.4, 128.0, 128.2, 139.9, 141.5.

#### ACKNOWLEDGEMENTS

This work was supported by grant NSF CHE-8314169 of the National Science Foundation. Acknowledgement is also made to the Donors of the Petroleum Research Fund, administered by the American Chemical Society, for support under grant 17171-AC1. We are grateful to Professor J. Phillip Bowen for assistance and advice concerning the force field calculations.

#### REFERENCES AND FOOTNOTES

1. Paper 48. E.L. Eliel and E.M. Olefirowicz, J.Comp.Chem., in press.
2. In part from the Ph.D. Dissertation of Edward M. Olefirowicz, 1987.
3. In part from the Ph.D. Dissertation of Maria T. Alvarez.
4. Present address: Department of Chemistry, University of Wyoming, Laramie, WY 82071.
5. cf. G. Solladié, G. Demailly, and C. Greck, Tetrahedron Lett., 1985, 26, 435; G. Solladié, C. Greck, G. Demailly, and A. Solladié-Cavallo, Tetrahedron Lett., 1982, 23, 5047.
6. M.T. Alvarez, Ph.D. Dissertation, University of North Carolina, Chapel Hill, NC, 1987.
7. This behavior is, of course, not unusual. For an extreme case, see E.L. Eliel and E. Brunet, Tetrahedron Lett., 1985, 26, 3421; E. Brunet and E.L. Eliel, J.Org.Chem., 1986, 51, 677.
8. J.T. Sprague, J.C. Tai, Y. Yuh, and N.L. Allinger, J.Comp.Chem., 1987, 8, 581.
9. The maximum distance at which hydrogen bonding is effective was taken to be the distance at which rotating H-O- away from O-S- caused no change in total energy, i.e. the distance at which electrostatic attraction exactly counterbalances van der Waals repulsion.
10. N.J. Leonard and C.R. Johnson, J.Org.Chem., 1962, 27, 282.
11. B.J. Graves and D.J. Hodgson, Acta Crystallog.Sect.B, 1982, 838, 135.
12. P.W.R. Corfield, R.J. Doedens, and J.A. Ibers, Inorg.Chem., 1967, 6, 197.
13. G. Germain, P. Main, and M.M. Woolfson, Acta Crystallogr.Sect.A, 1971, A27, 368.
14. Tables of hydrogen atom parameters, anisotropic thermal parameters and listings of observed and calculated structure amplitudes have been deposited with the Cambridge Crystallographic Data Centre, University Chemical Laboratory, Lensfield Road, Cambridge, CB2 1EW, UK.

Received, 5th September, 1988